Geomorphology xxx (2015) xxx–xxx

Contents lists available at ScienceDirect

Geomorphology

journal homepage: www.elsevier.com/locate/geomorph

Paleoflood discharge reconstruction in Tatra Mountain streams

Juan Antonio Ballesteros-Cánovas [a,b,*], Markus Stoffel [a,b,c], Barbara Spyt [d], Karolina Janecka [d], Ryszard J. Kaczka [d], Michał Lempa [d]

[a] Dendrolab.ch, Institute of Geological Sciences, University of Berne, CH-3012 Berne, Switzerland
[b] Climatic Change and Climate Impacts, Institute for Environmental Sciences, University of Geneva, CH-1205 Geneva, Switzerland
[c] Department of Earth Sciences, University of Geneva, CH-1205 Geneva, Switzerland
[d] Faculty of Earth Sciences, University of Silesia, PL-40007 Katowice, Poland

ARTICLE INFO

Article history:
Received 22 June 2015
Received in revised form 3 December 2015
Accepted 10 December 2015
Available online xxxx

Keywords:
Paleoflood
Dendrogeomorphology
Flood
Tatra Mountains

ABSTRACT

Floods represent a common process in Tatra Mountain streams and may cause flood risk in the valleys of the Tatra foreland. Dealing with the hazards and risks caused by floods requires a detailed analysis of the frequency and magnitude of past and recent events. However, the Polish Tatra region is characterized by a scarcity of data on past floods in general and on systematic peak discharge in particular. In this study, we performed a paleohydrological analyses in four high-gradient mountain streams using scarred trees as paleostage indicators. We couple two-dimensional hydraulic modelling in a highly-resolved topographic environment (LiDAR data) with an important spatiotemporal data set of scars on trees to investigate (i) the magnitude of unrecorded major floods of the twentieth century, (ii) the effect of variability in geomorphic tree positions on the peak discharge reconstruction, and (iii) the impact of reconstructed events on the results of flood frequency analyses. The data set is based on a total of 55 scarred trees and allows peak discharge reconstruction of 16 major floods covering the last 113 years. Results suggest that trees growing in straight stream reaches or in the inner side of channel bends would be better candidates for peak discharge reconstructions than trees located on the outer side of channel bends or growing in overbank sections with dense vegetation cover. The largest reconstructed flood is dated to 1903 with an estimated peak discharge of 115.9 ± 59.2 $m^3 s^{-1}$, and larger-than-today floods are found to have occurred at Strążyska and Łysa Polana in the first half of the twentieth century. The inclusion of our results into the flood frequency analyses suggests that flood hazards might have been underestimated by up to 25.5% in the case of a 100-year flood in Strążyski Stream. In that sense, our findings will be useful for the design of future strategies dealing with flood risks in the foreland of the Polish Tatra Mountains.

1. Introduction

Mountain streams have steep channels and are characterized by recurrent, highly-turbulent and sediment-laden flows (Wohl, 2000, 2006). Their quick hydrological response as well as their considerable power (Borga et al., 2014) make mountain streams highly hazardous and events therein difficult to forecast (Marchi et al., 2010; Borga et al., 2011) such that they cause large amounts of losses and fatalities worldwide. Floods in mountain environments are related to catchment disposition, channel characteristics, and climate triggers (Blöschl et al., 2015), with the last being expected to change in the course of the next few decades with very direct and potentially drastic impacts on precipitation regimes (Kundzewicz et al., 2010).

In view of the ongoing climate changes and expected impacts on process activity, the assessment of flood hazard and risk in mountain areas will require an improved understanding of their spatiotemporal occurrence as well as their links and drivers to climate (Merz et al., 2014). An improved understanding of past and expected states and/or changes of the magnitude (i.e., peak discharge) as well as the return period of flood (Enzel et al., 1993; Lang et al., 1999; Baker, 2008) is not only critically needed for the management of riparian zones downstream of the headwater systems but also the design of reliable mitigation channel infrastructures such as artificial channels or dikes. The main drawback in analysing mountain streams is, however, related to the lack of past observations and measurements. As a consequence, the scarcity of systematic data or the shortness of existing records typically hamper the analysis of reliable and representative flood events, which in turn affects the flood hazard assessment (Sigafoos, 1964; Ballesteros-Cánovas et al., 2013, 2015a; Bodoque et al., 2015).

The Polish Tatra Mountain streams are a paradigm of this problem. In this region, the inhabited valleys in the northern foothills of the Tatras are subjected to frequent floods triggered mainly by intense and long-lasting precipitation during summer (Niedźwiedź et al., 2015). As the network of available gauging stations in the area is not only highly

* Corresponding author at: Dendrolab.ch, Institute of Geological Sciences, University of Berne, CH-3012 Berne, Switzerland.
E-mail address: juan.ballesteros@dendrolab.ch (J.A. Ballesteros-Cánovas).

http://dx.doi.org/10.1016/j.geomorph.2015.12.004
0169-555X/

discontinuous, but also short operating and not really representative enough for a proper hydrological characterization (Kundzewicz et al., 2014; Ballesteros-Cánovas et al., 2015b,c), we were obliged to carry out alternative and complementary approaches to improve existing understanding of potential flood events in the area (Kundzewicz et al., 2014).

Botanical evidence represents a valuable resource to date and quantifies the magnitude of past flood events in streams with only poorly gauged data (Stoffel and Wilford, 2012; Ballesteros-Cánovas et al., 2015a) and thus allows extension of existing flow records, which may in turn improve the estimation of flood frequency distributions (FFD; O'Connor et al., 1994; O'Connell, 2005). Scars on trees result from the impact of and abrasion by sediment and woody debris transported during floods and have been described as being one of the most useful paleostage indicators (PSI) for peak discharge reconstructions (Yanosky and Jarrett, 2002; Baker, 2008). This scar-based approach is founded on a trial-and-error approximation between scar height and modelled water table profiles as obtained from hydraulic models (Jarrett and England, 2002; Yanosky and Jarrett, 2002; Ballesteros-Cánovas et al., 2015a). The reliability of scar-based peak discharge reconstruction has been proven over the past decades (McCord, 1996; Corriell, 2002; Yanosky and Jarrett, 2002; Ballesteros-Cánovas et al., 2011a,b). For instance, Smith and Reynolds (1983) observed that the average differences between the height of ice-flood scar and punctual flow gauge records along the Red Deer River amounted to 1.37 ± 0.94 m. By estimating the peak discharge of past flood events in two mountain streams in Arizona and Colorado (USA), McCord (1996) compared reconstructions with existing flow records and suggested that scar height could represent minimum flow stages. Observations from Gottesfeld (1996) in the Skeena River (USA) suggest that scar heights were closely related to maximum flood stage (within 20 cm), exhibiting a slope close to the water-surface slope at peak discharge. In the case of high-gradient streams, Yanosky and Jarrett (2002) documented a range of differences between scar heights and high-water marks (HWM) ranging between −0.6 and 1.5 m. Similar ranges of uncertainties have recently been suggested by Ballesteros-Cánovas et al. (2011a; −0.8 to 1.3 m) who also distinguished large from small scars. The same authors also highlighted the need to take critical sections with stable bedrock condition as well as sections with specific hydraulic conditions (i.e., transaction between different hydraulic phases) into account. These discrepancies between maximum flow stage as defined by HWM and scar heights observed in trees have been related to tree position and hydraulic flow conditions (Gottesfeld, 1996; Yanosky and Jarrett, 2002; Ballesteros-Cánovas et al., 2011a,b).

In this paper, we present a scar-based paleoflood discharge reconstruction for four poorly or ungauged mountain streams in the Tatra Mountains (Poland). Based on a comparably large number of scarred trees, two-dimensional hydraulic model and highly-resolved LiDAR data, we focus on (i) the quantification of past flood magnitudes, (ii) the definition of the most suitable geomorphic locations from which trees should be sampled for peak discharge reconstruction based on PSI (i.e., scar heights), and (iii) the comparison of existing flow discharge series for the region with the reconstructed events.

2. Study area

The peak discharge reconstruction was conducted in four different mountain streams draining the northern slopes of the Polish Tatra Mountains (Fig. 1; Table 1). Catchments and stream reaches were selected according to (i) their spatial and hydrogeomorphic representativeness of the region, (ii) the availability of flow gauge records, and (iii) their potential for dendrogeomorphic studies (i.e., presence of trees with PSI and limited human disturbance in the form of path networks or forestry). All the catchments contribute to the main foreland rivers for which a long record of flood damage exists for the last two centuries (Kotarba, 2004; Kundzewicz et al., 2014; Ballesteros-Cánovas et al., 2015b).

Catchment geology consists of a crystalline and metamorphic core overlain by Mesozoic sedimentary rocks. Characteristic geomorphic features of the area comprise — but are not limited to — Pleistocene glacial and Holocene mass-movement forms and deposits including glacier abrasion, glacier lakes, moraine deposits, and alluvial/colluvial fans. Vegetation is mainly characterized by five climatic-vegetation zones (Niedzwiedz, 1992), with timberline being located at around 1420 m asl. The high-elevation study reaches Rybi Potok (RP), Roztoka (DR), and Chochołowski Potok (DCH) are located in the cool temperate belts characterized by the presence of Norway spruce (*Picea abies* (L.) Karst.), whereas the low-elevation reach of Strążyski Potok (ST) is located in a cool temperate belt characterized by a mixed forest of *P. abies* and Silver fir (*Abies alba* Mill.). The channels of RP, DR, and DCH have been formed in granitic and pegmatitic bedrock (Bac-Moszaszwili et al., 1979) covered by gravel and loamy moraine deposits. By contrast, ST flows on sedimentary rocks. All four reaches have a straight and/or braided channel pattern and a channel bed composed of pebble-cobble material with sporadic boulders. Lateral gravel bars as well as woody debris are common in all reaches, whereas mid-channel bars were limited to DCH. Abundant bank undercuts and secondary channels testify to the presence of past fluvial activity and related flood events. Table 1 summarizes the main characteristics of the analysed stream reaches.

A limited number of hydroclimatic series exist in the study area. The oldest instrumental data date back to the end of the nineteenth century, when gauges were, however, frequently moved or working for only a few years. The two world wars during the twentieth century caused yet another gap in measurements. Table 1 provides information on available data and the length of records.

From a climatic perspective, the Tatra Mountains form a barrier for air mass movement and in particular for polar marine air masses (65%) and polar continental air masses (25%) that make up 90% of the events being blocked by the chain (Niedźwiedź et al., 2015). The blocking effect often results in heavy rainfall events with 24-h precipitation sums of up to 300 mm (30 June 1973; Niedźwiedź et al., 2015). Annual precipitation, therefore, varies from 1100 mm at the foothills (Zakopane, 844 m asl) to 1660 mm at timberline (Hala Gąsienicowa, 1550 m asl) and 1721 mm on the summits (Lomnicky, 2635 m asl). The most effective precipitation events resulting in floods are concentrated in the summer season (Niedźwiedź et al., 2015; Ruiz-Villanueva et al., 2014; Ballesteros-Cánovas et al., 2015b), with maximum recorded peak discharges of up to 144 $m^3 s^{-1}$ downstream RP and DR, 88 $m^3 s^{-1}$ at DCH, and 6 $m^3 s^{-1}$ at ST.

Over the last three centuries, the study region was affected by intense human activity in the form of pasturing and intense logging in the eighteenth and nineteenth centuries. Grazing pressure in the upper parts of the catchments has been particularly intense during the nineteenth and mid-twentieth centuries. Both impacts have altered soil and vegetation characteristics, resulting in increased flooding. The Tatra National Park was enacted in 1954, also to reduce the negative effect that altered soils and vegetation had on floods, but pasturing locally continued until 1978 and logging also remains permitted under certain conditions.

3. Methodology

3.1. Scarred trees analysis

All *P. abies* and *A. alba* trees presenting visible flood scars or evidence of internal tree damage were sampled and dated following the standard dendrogeomorphic sampling procedures as described by Stoffel and Corona (2014). These procedures consisted of (i) sampling of injured trees using an increment borer, (ii) sample preparation in the lab (mounting, sanding), (iii) tree-ring dating, (iv) detection of growth

Please cite this article as: Ballesteros-Cánovas, J.A., et al., Paleoflood discharge reconstruction in Tatra Mountain streams, Geomorphology (2015), http://dx.doi.org/10.1016/j.geomorph.2015.12.004

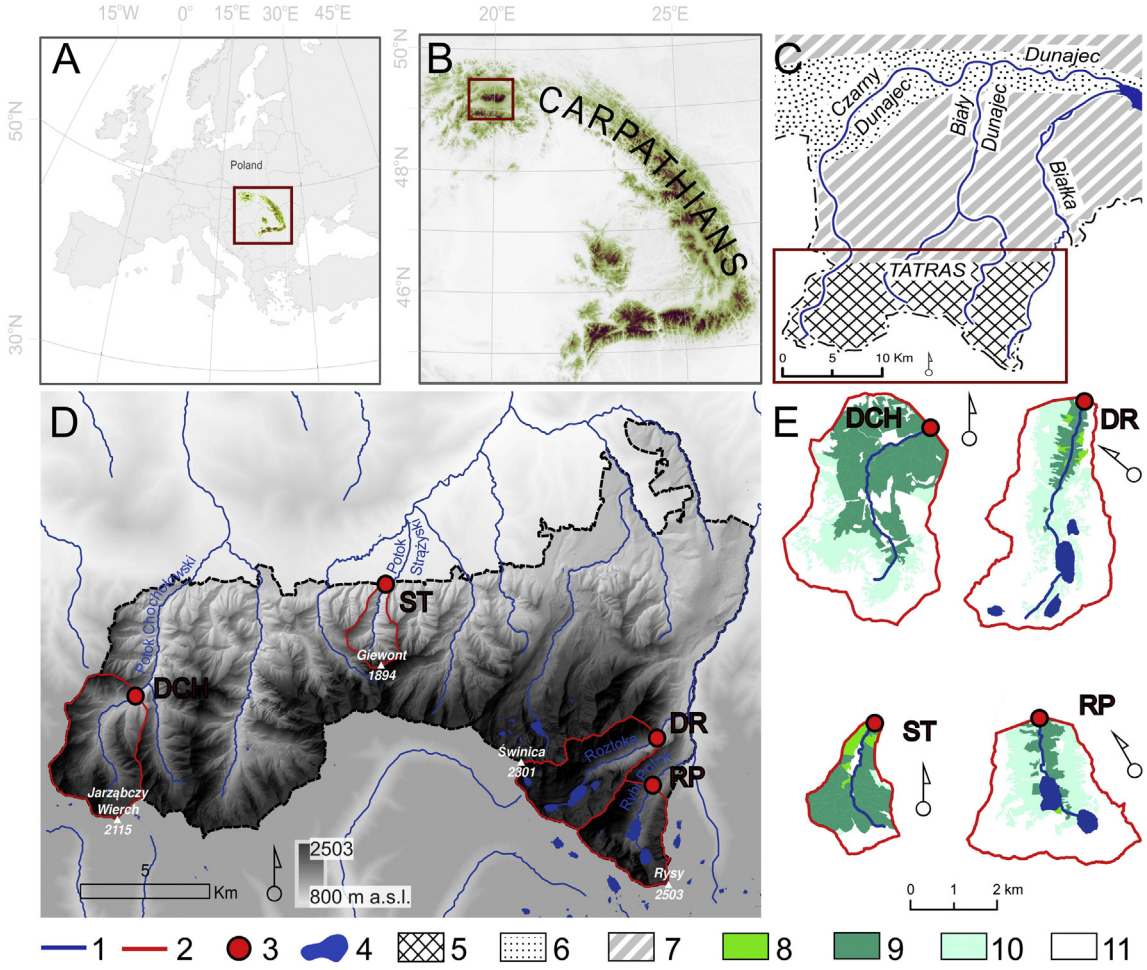

Fig. 1. Location of the Tatra Mountains within Europe (A) and the Carpathian Arc (B) and main physiogeographic regions of the Polish Tatra Mountains and their foreland (C). Location of the four studied reaches (D) with predominant land use patterns of the study catchments (E). DCH — Chochołowski Stream; ST — Strążyski Stream; DR — Roztoka Stream; and RP — Rybi Potok Stream. 1 — Streams; 2 — catchments analysed in this study; 3 — locations of the study sites; 4 — lakes; 5 — high mountains; 6 — intramontane and submontane depressions; 7 — intermediate and low mountains; 8 — deciduous forest; 9 — coniferous forest; 10 — dwarf pine shrubs; 11 — low vegetation.

anomalies, and (v) definition of past flood events. A detailed description of individual steps carried out for flood dating in the study reaches described in this paper can be found in Ballesteros-Cánovas et al. (2015b). Only trustworthy scars that could be attributed clearly to past flood events were considered for peak discharge reconstruction. The criteria used included (i) scars belonging to dated past flood events for which a much larger number of samples was available (see Ballesteros-Cánovas et al., 2015a, for details on the dating procedures used); (ii) scars facing the direction of flow and (iii) exhibiting a shape typical of flood impacts (see Ballesteros-Cánovas et al., 2010,

Table 1
Main catchment and stream reach characteristics.

			DCH	ST	DR	RP
Catchment level	Aspect		NNW	NNW	NW	NW
	Area (km^2)		13.84	3.69	11.79	8.64
	Flood concentration time (h)		0.43	0.26	–	–
	Land cover (km^2, %)	Forested	5.51 (40%)	2.89 (79%)	1.02 (9%)	0.88 (10%)
		Un-forested	5.64 (40%)	0.71 (21%)	7.37 (62%)	4.68 (55%)
		Dwarf pine zone	2.74 (20%)	–	2.80 (24%)	2.52 (29%)
		Glacier lakes	–	–	0.63 (5%)	0.52 (6%)
	Geological characteristics		Crystalline (80%), moraine deposits	Carbonates (100%)	Crystalline (70%), moraine deposits (30%)	Crystalline (80%), moraine deposits (20%)
Reach level	Stream length (km)		5.1	3.3	5.9	2.9
	Average slope (%)		4	5	13	9
	Stream order		Fourth	Second	Second	Second
	Vegetation		*P. abies*	*P. abies* and *A. alba*	*P. abies*	*P. abies*
	Systematic records (type and time covered)		Polana Chochołowska: (rainfall: 1971–1981) Kojsówka: (water stage: 1963–1983; discharge: 1971–1983)	Strążyski: (water stage: 1964–1983; discharge: 1971–1983) Zakopane: (rainfall 1954–2011)	Morskie Oko: (rainfall: 1982–2004) Roztoka: (water stage: 1922, 1923, 1925, 1926)	Morskie Oko: (rainfall: 1982–2004) Łysa Polana: (rainfall: 1955–1979; water stage: 1924, 1927–1931, 1948–2011; discharge: 1961–1983)

Please cite this article as: Ballesteros-Cánovas, J.A., et al., Paleoflood discharge reconstruction in Tatra Mountain streams, Geomorphology (2015), http://dx.doi.org/10.1016/j.geomorph.2015.12.004

2015a; Trappmann and Stoffel, 2015 for details). Therefore, we discarded all areas where the impact of human activity was clearly visible, or where geomorphic processes other than floods and/or debris flows (e.g., snow avalanches, rockfalls) might have caused scarring of trees. We also excluded those river reaches from the evidence of intense bankfull destabilization.

In the field, the position of trees showing PSI was recorded with a GPS (Trimble GeoXT 6000, precision <1 m). In addition, we used a laser distance metre (TruePulse 360°B, precision: 30 cm) to measure the distance of trees with respect to the thalweg as well as scar height (i.e., its central height). We also defined trees according to (i) their position with respect to the *main channel*, *bankfull border* or *overbank* deposits; (ii) their position within *straight reaches*, *internal* or *external* side of a channel bend; or (iii) as *exposed trees* in case they were growing without any obstacles (trees, boulders, etc.) within 5 m upstream (Fig. 2).

3.2. Hydraulic modelling

The two-dimensional hydrodynamic model *IBER* (www.iberaula.es) was used to model water depth and flow velocities in the study reaches. IBER simulates turbulent-free, unsteady surface flows and environmental processes in rivers by solving depth-averaged two-dimensional shallow water (2D Saint-Venant) equations using a finite volume method with a second-order roe scheme. This method is particularly suitable for flows in mountain streams where shocks and discontinuities can occur and flow hydrographs tend to be very sharp. The method is conservative, even in cases where wetting and drying processes occur. The model works in a nonstructured mesh consisting of triangles or quadrilateral elements. For this specific study, we used LiDAR data (1×1 m resolution) as a mesh basis. Bed friction is evaluated using Manning's n roughness coefficient, which was initially assessed in the field by using homogenous roughness units (Chow, 1959). In this study we use a Manning's n of 0.04 for the main channel and 0.1 for the overbank sections. To compute inlet water discharge (steady flow) into each study reach, we modelled successive inlet water discharges. Based on the output of the hydraulic model, a peak discharge (q)–water stage (W) relationship W (q, i) was obtained for each scarred tree (i). We used the mean and standard deviation to estimate average peak discharge of each flood event.

3.3. Flow series analysis

In terms of flow series analysis, we initially performed a descriptive statistical analysis of available flow gauge series (Fig. 3). The reconstructed magnitude of past floods was then added to the existing flow gauge series as nonsystematic data using Bayesian Markov Monte Carlo Chain algorithms (Gaume et al., 2010). To this end, we used the freely available R package nsRFA (Viglione et al., 2013). The procedure is based on the likelihood of the available data set merging with nonsystematic data for quantile estimation, taking into account the existing and quantified uncertainties. We used the generalized extreme value distribution (GEV) to derive the flood quantiles at each of the studied catchments. In the flood frequency analyses, reconstructed peak discharges were included as a range of value (min–max, DB type), so as to include uncertainties in the reconstruction. The robustness of this method has been tested previously in other mountain regions (Gaume et al., 2010; Ruiz-Villanueva et al., 2013). A detailed theoretical and practical description of the procedure followed in this paper can be found in Gaál et al. (2010). Finally, we compared the obtained flood quantiles for 10-year and 100-year return periods, as well as their related uncertainties, from the flood frequency analysis considering systematic series and nonsystematic data.

4. Results

4.1. Flood scars

Table 2 shows the main characteristics of scarred trees considered for peak discharge reconstruction. A total of 55 trees showed visible scars inflicted by sediment and wood transported during past flood events (namely 25 in DCH, 22 in RP, 6 in ST, and 3 in DR). The scar dating points to 16 past events for which the suite of usable scars is large enough for peak-discharge estimation. Concretely, scars provide evidence for 7 well-replicated flood events in DCH, 6 in RP, 3 in ST, and 1 in DR. The oldest of these dated events goes back to 1903 in RP, whereas the latest event on record took place in DCH in 2002. Only the well-known event of 1934 (which caused substantial flooding in the foothills and lowlands) was common for DCH and ST, whereas the remaining 17 events were only recorded in one of the three streams. On average, the stream reach showing the highest PSI was DCH (104.1 ± 38.1 cm above the thalweg), whereas lower PSI were found in DR (56.6 ± 24.6 cm). In most cases, scarred trees were found in straight channel reaches, (S; except for RP which is characterized by a sinuous channel course), on the bankfull channel boundary (B), or within the main channel (C). In DCH and ST, scarred trees were mostly placed at sites which are obviously exposed to the flow (E) or at least in positions lacking trees immediately upstream (I), whereas in RP and DR scarred trees were most frequently observed in highly forested sites (D). Reconstructed events coincide with high flows in existing gauge-station records. We found three matches with DCH and ST, whereas only one match was identified with RP and DR flow records.

4.2. Scar-based flood discharge reconstruction

Fig. 4 shows the graphical output of the largest flood reconstructed with IBER for each of the streams, whereas Table 3 provides estimated discharge values for the reconstructed flood events. The largest

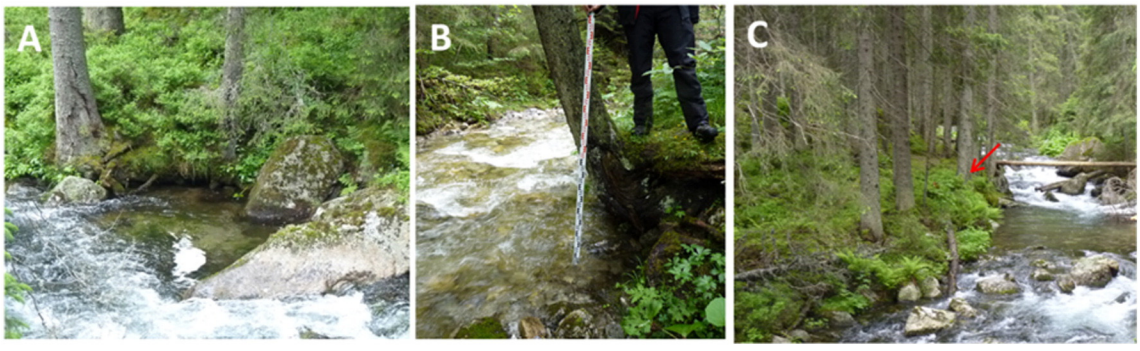

Fig. 2. Examples of scarred trees located in the study reaches. Examples (A) and (B) represent trees exposed to the flow but without other trees growing immediately upstream. Example (C) represents a scarred tree in a densely forested patch. In all cases, trees grow at the boundary of the bankfull channel.

Please cite this article as: Ballesteros-Cánovas, J.A., et al., Paleoflood discharge reconstruction in Tatra Mountain streams, Geomorphology (2015), http://dx.doi.org/10.1016/j.geomorph.2015.12.004

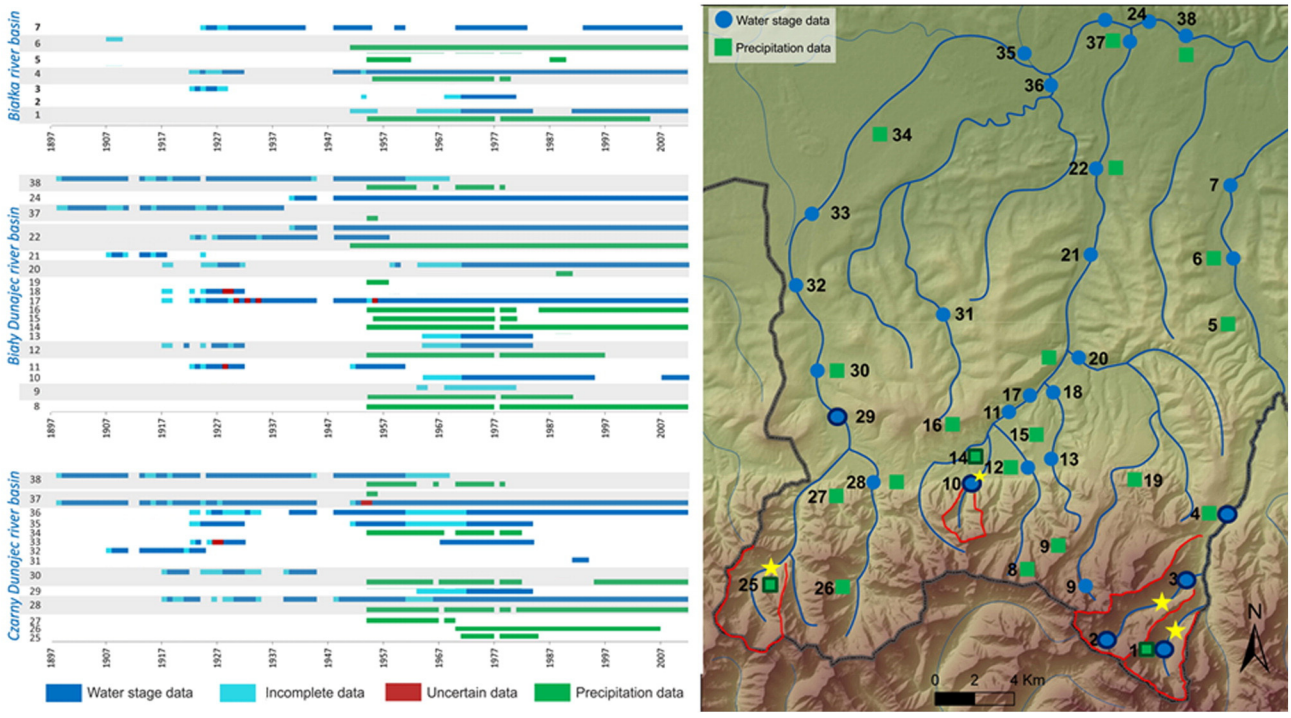

Fig. 3. Spatial and temporal distribution of available meteorological and hydrological data sets on the northern slopes of the Tatra Mountains and on their foreland.

reconstructed event occurred in RP in 1903 with a discharge of 115.9 ± 59.2 $m^3 s^{-1}$, whereas the smallest event is reconstructed in ST in 1934 with 11.1 ± 4.9 $m^3 s^{-1}$. The only flood event identified for more than one catchment is dated to 1934 and caused reconstructed discharges of 39.7 ± 11.8 and 11.1 ± 4.9 $m^3 s^{-1}$ in DCH and ST, respectively).

The ranges of discharges for reconstructed events were generally much higher in DCH and RP (92.8 to 39.7 and 115.9 to 28.6 $m^3 s^{-1}$, respectively) than in ST (45.8–11.1 $m^3 s^{-1}$) and DR (24.1 ± 7.6 $m^3 s^{-1}$). Noteworthy, the average standard deviation in reconstructed peak discharges was almost 41%, with the lowest deviation observed in DCH in 1983 (~16%). By contrast, the largest deviation (up to 80%) was found for the 1997 event in ST. Detailed evaluation of discharge deviations for years with more than three scars (i.e., 1926, 1956, 1958, 1963, 1972, and 1990; Fig. 5) shows that trees with lower variability in scar heights were located (i) in sections with straight channel or the internal side of channel bends (10–20%), (ii) far away from neighbouring trees (23%), or (iii) next to the boundary of bankfull channel (~20%). Trees showing the largest variability in scar heights were, by contrast, located on the external side of channel bends (up to 40%), in areas with high tree density (41%) as well as within the central channel or in overbank positions (up 30%).

4.3. Flood frequency

Fig. 6 provides a comparison between nonsystematic (i.e. tree-ring records) and systematic (i.e. flow gauge data) data for each of the studied streams. The Strążyska flow gauge station (ST) is located 1 km upstream of the study reach of the same name. Available flow records cover the periods 1971–1994 and 2007–2011. Average recorded discharge is 2.9 ± 2.6 $m^3 s^{-1}$ with a variance (VAR) of 7.1 and kurtosis (K) of 16.5, whereas the average reconstructed discharge for events between 1934 and 1952 amounts to 17.5 ± 11.9 $m^3 s^{-1}$.

The Łysa Polana flow-gauge station (LY) is located 7 km downstream of RP and recorded runoff from DR and from another catchment located to the east for the period 1961–2011. Average recorded flow discharge is 37.2 ± 26.7 $m^3 s^{-1}$ (VAR = 7.4; K = 6.6), whereas average discharge

Table 2
Characteristics of the scars used as paleostage indicators (PSI) for each of the studied stream reaches. Abbreviations: S — straight reaches; EM — external side of channel bends; IM — internal side of channel bends; D — trees growing on dense forest patch with obstacles around (5 m); E — trees growing on dense forest patch but exposed to the flow; I — Isolated trees; B — trees growing at the boundary of the bankfull channel; C — trees growing in the channel; OB — trees growing on the floodplain.[a]a

Stream	Scars (nb)	Dating (*)	h scars (cm)	Tree position (%)	Flow gauge station
DCH	25	1934(2), 1955(4), 1963(4), 1972(8), 1983(3), 1991(2), 2002(2)	104.1 ± 38.1	S = 72, EM = 20, IM = 8 E = 12, I = 52, D = 36 B = 40, C = 24, OB = 36	1963, 1972 and 1983 −9.5 km downstream
ST	10	1938(2), 1947(2), 1952(2)	75.0 ± 15.1	S = 50, EM = 30, IM = 20 E = 30, I = 30, D = 40 B = 30, C = 50, OB = 10	1970, 1976 and 1983 1 km upstream
RP	22	1903(2), 1926(5), 1949(2), 1958(8), 1970(2)	94.8 ± 40.9	S = 4, EM = 48, IM = 48 D = 100 B = 66, C = 14, OB = 20	1970 1 km upstream
DR	3	1990	56.6 ± 24.6	S = 100 D = 100 B = 66, C = 34	1990 7 km downstream

[a] Note: All flood events have been dated based on a large number of samples with different disturbance typologies, where the weighted index (Wit) ranked between 0.6 and 8.26 for DCH, 1.07 and 4 for ST, and 0.55 and 32.2 for DR (all events satisfied the threshold number of growth disturbance >2 and Wit >0.5; see Ballesteros-Cánovas et al., 2015b).

Please cite this article as: Ballesteros-Cánovas, J.A., et al., Paleoflood discharge reconstruction in Tatra Mountain streams, Geomorphology (2015), http://dx.doi.org/10.1016/j.geomorph.2015.12.004

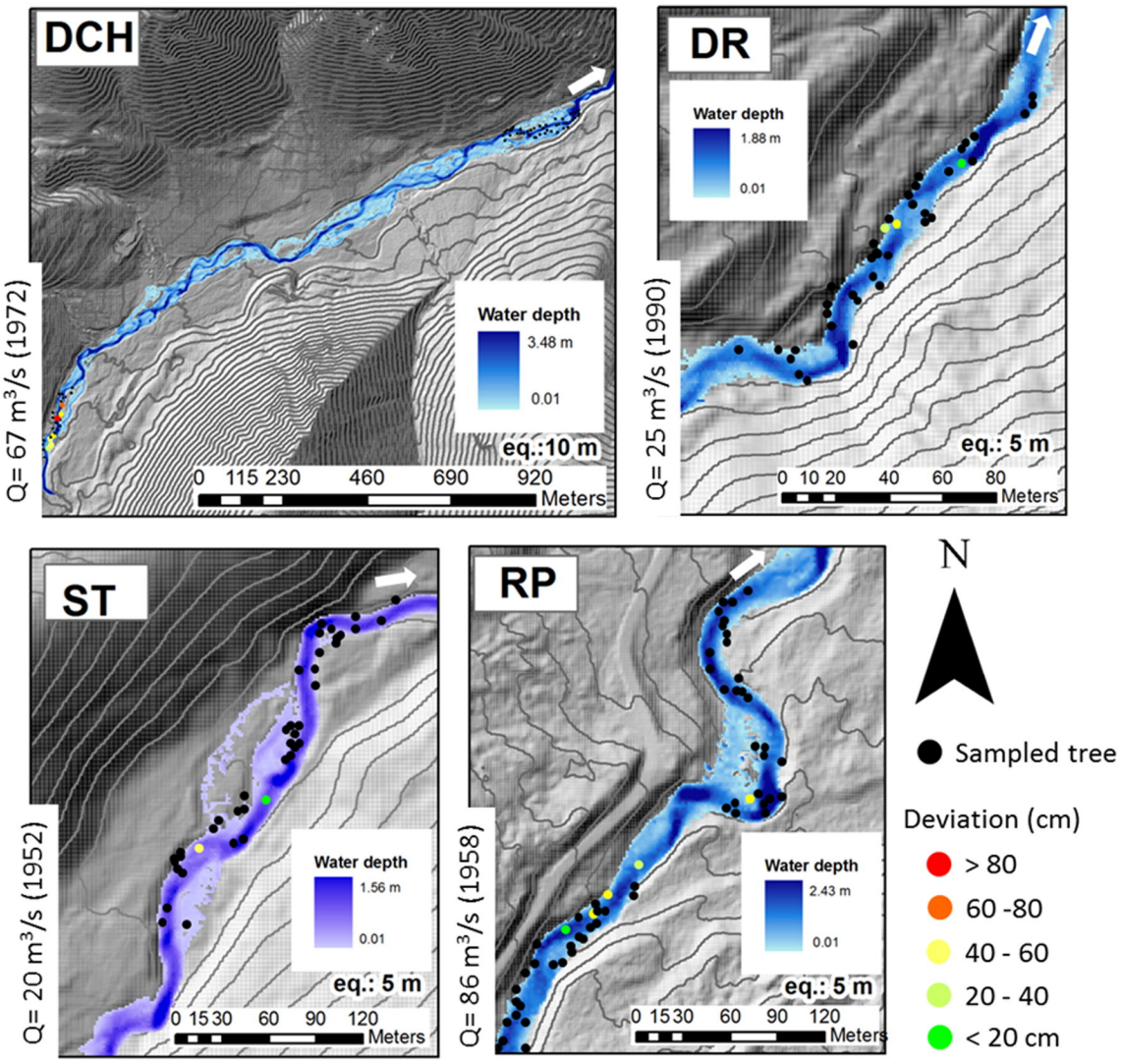

Fig. 4. Modelled water depths in the four study reaches during particular flood events of the twentieth century. Discharge was defined in a trial-and-error approach aiming at minimization of the difference between observed scar heights and modelled flow levels.

during reconstructed events between 1903 and 1970 was 72.1 ± 85.8 $m^3 s^{-1}$. The only recorded flood in DR took place in 1990 and was estimated at 24.1 ± 7.6 $m^3 s^{-1}$. The reconstructed events of 1970 in RP (39.6 ± 9.5 $m^3 s^{-1}$) and of 1990 in DR (24.1 ± 7.6 $m^3 s^{-1}$) have been registered by the flow-gauge station with peak discharges of 30.2 and 22.4 $m^3 s^{-1}$, respectively, and thus point to the high potential and reasonable accuracy of paleodischarge values as obtained with tree-ring proxies.

The Kojsówka flow-gauge station (KO) is located 9.5 km downstream of site DCH and recorded runoff from two more catchments. Available flow records exist for the period 1963–1983. The average recorded annual maximum discharge during this period was 37.6 ± 21.0 $m^3 s^{-1}$ (VAR = 442.0; K = 2.96). By contrast, the average of reconstructed flood events at DCH for the period 1934–2002 was estimated at 55.4 ± 54.4 $m^3 s^{-1}$. Three flood events for which both datasets exist were 92.8 ± 25.1 (1963), 67.8 ± 28.9 (1972), and 46.7 ± 7.9 $m^3 s^{-1}$ (1983) as compared to 29.6, 61 and 25.4 $m^3 s^{-1}$, respectively, thus pointing to a good agreement for the event in 1972 and substantial differences between the series for the events of 1963 and 1983.

Because of the proximity between the study area and the gauging station, the FFA analysis has focused on ST. Changes in the estimated flood frequency distribution (maximum annual discharge) including systematic series and nonsystematic data are graphically shown in Fig. 7 and quantified in Table 4. The observed changes in Q_{mean} between an assessment based exclusively on systematic data for ST and those seen in a series with paleodischarge data ranked between 10% and 25.5% for T = 10 years and T = 100 years, respectively. Additionally, the uncertainties after inclusion of paleodischarge data decrease about 39.1% and 47.3%, for T = 10 years and T = 100 years, respectively.

5. Discussion

In the study, we provided a scar-based flow discharge reconstruction for four headwater streams on the northern slopes of the Tatra Mountains (southern Poland) for the period 1903–2012. We analysed 55 scarred trees and used a two-dimensional hydraulic model run on highly resolved topography to estimate peak discharge of 16 unrecorded flood events. Moreover, we investigated the role of relative tree position on flow discharge reconstructions, before we quantify changes in flood frequency values as a result of the inclusion of nonsystematic data in recorded series.

5.1. Reliability of the scar-based peak discharge reconstruction

This study represents the longest flood discharge reconstruction in the Tatra Mountains and complements short and discontinuous flow

Please cite this article as: Ballesteros-Cánovas, J.A., et al., Paleoflood discharge reconstruction in Tatra Mountain streams, Geomorphology (2015), http://dx.doi.org/10.1016/j.geomorph.2015.12.004

Table 3
Peak discharge reconstructions based on scar heights and water levels as modelled for each stream reach and each reconstructed (i.e. tree-ring data) event considered. EPD — estimated peak discharge at each tree location, RPD — reconstructed peak discharge for specific event.

Site	Year	Scar height (cm)	EPD ($m^3 s^{-1}$)	RPD ($m^3 s^{-1}$)	Site	Year	Scar height (cm)	EPD ($m^3 s^{-1}$)	PD ($m^3 s^{-1}$)
DCH	1934	70	48.1	39.7 ± 11.8	RP	1970	90	21.9	39.6 ± 9.5
DCH	1934	170	31.3		RP	1970	80	35.3	
DCH	1955	90	29.0	56.0 ± 23.9	RP	1903	80	74.0	115.9 ± 59.2
DCH	1955	130	45.3		RP	1903	190	157.8	
DCH	1955	90	83.7		RP	1949	140	71.8	59.4 ± 17.5
DCH	1955	90	66.1		RP	1949	40	47.0	
DCH	1963	110	69.8	92.8 ± 25.1	RP	1926	118	114.1	70.4 ± 34.6
DCH	1963	120	89.1		RP	1926	110	70.7	
DCH	1963	100	119.6		RP	1926	90	67.3	
DCH	1972	125	65.1	67.8 ± 28.9	RP	1926	50	29.7	
DCH	1972	115	83.5		RP	1958	90	52.3	86.2 ± 47.7
DCH	1972	130	58.5		RP	1958	100	47.8	
DCH	1972	50	29.2		RP	1958	90	82.1	
DCH	1972	100	39.4		RP	1958	70	162.8	
DCH	1972	155	86.1		RP	1958	120	59.5	
DCH	1972	60	113.2						
DCH	1983	120	52.3	46.7 ± 7.9	ST	1938	80	14.5	11.1 ± 4.9
DCH	1983	105	41.1		ST	1938	90	7.6	
DCH	1991	60	28	44.8 ± 23.7	ST	1947	80	14.5	20.7 ± 8.8
DCH	1991	70	61.5		ST	1947	50	53.4	
DCH	2002	30	31.2	40.4 ± 12.8	ST	1952	80	25.4	20.8 ± 6.5
DCH	2002	50	49.4		ST	1952	80	16.2	
DR	1990	85	44.8	24.1 ± 7.6					
DR	1990	40	19.1						
DR	1990	45	8.4						

records of gauge stations. Comparison between flow records and estimated discharge at ST is not possible as the short gauge series and reconstructed events did not occur during the same periods or did not cause impacts. However, floods recorded at the KO and LP gauge stations, located 7.5 and 9 km downstream of the study sites, respectively, agreed with reconstructed flow discharges. For instance, for 1972 and 1983 at our study site DCH, we obtained peak discharges of 67.8 ± 28.9 and 46.7 ± 7.9 $m^3 s^{-1}$ respectively, whereas at the KJ gauge station we recorded 61 and 26 $m^3 s^{-1}$. In a similar way, the floods reconstructed for 1970 and 1990 at study sites RP and DR were estimated at 39.6 ± 9.5 and 24.1 ± 7.6 $m^3 s^{-1}$, whereas the LP gauge station recorded for the same events 101 and 30.3 $m^3 s^{-1}$, respectively. With the exception of the flood in DCH in 1972, all reconstructed peak discharges were smaller than peak flow measured at the downstream gauge station, which can be explained by differences in the catchment areas and thus confirms the reliability of reconstructed discharge values (Williams, 1978; Knighton, 2014). However, this also means that the discharge reconstructed for the 1972 flood can be overestimated.

Despite the fact that scar-based flow discharge reconstructions were successfully tested in various mountain streams of the northern hemisphere in the past (Egginton and Day, 1977; Gottesfeld, 1996; Yanosky and Jarrett, 2002; Ballesteros-Cánovas et al., 2011a,b), we would like to stress that their reliability can still be limited as a result of uncertainties inherent to the approach. First, channel bed stability is normally given at critical sections but not elsewhere in the channel (Webb and Jarrett, 2002; Ballesteros-Cánovas et al., 2011a; Bodoque et al., 2015) such that inaccuracies in the estimation can occur in topography and thus in hydraulic computation. We have tried to avoid this problem by focusing on bedrock channels where stable bed topography can be guaranteed over periods of several centuries (Ballesteros-Cánovas et al., 2011a). Bedrock channel sections were present in ST, and semistable conditions were encountered in the case of RP and DR streams where big boulders control the vertical and horizontal stability of the channels. The channel at DCH was partly controlled by the presence of a bridge at the lower end of the study reach. The hydrological criteria of channel stability (Wyżga, 1997) remain, however, difficult to compute because

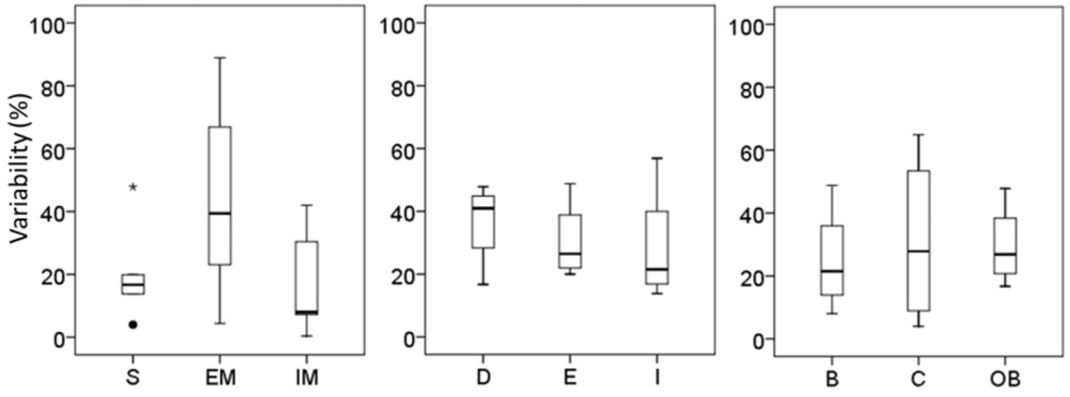

Fig. 5. Relationship between tree position and observed variability (in %) in peak discharge estimations. Trees location: S — straight reaches; EM — external side of channel bends; IM — internal side of channel bends; D — trees growing on dense forest patch with obstacles around (5 m); E — trees growing on dense forest patch but exposed to the flow; I — isolated trees; B — trees growing at the boundary of the bankfull channel; C — trees growing in the channel; OB — trees growing on the floodplain.

Please cite this article as: Ballesteros-Cánovas, J.A., et al., Paleoflood discharge reconstruction in Tatra Mountain streams, Geomorphology (2015), http://dx.doi.org/10.1016/j.geomorph.2015.12.004

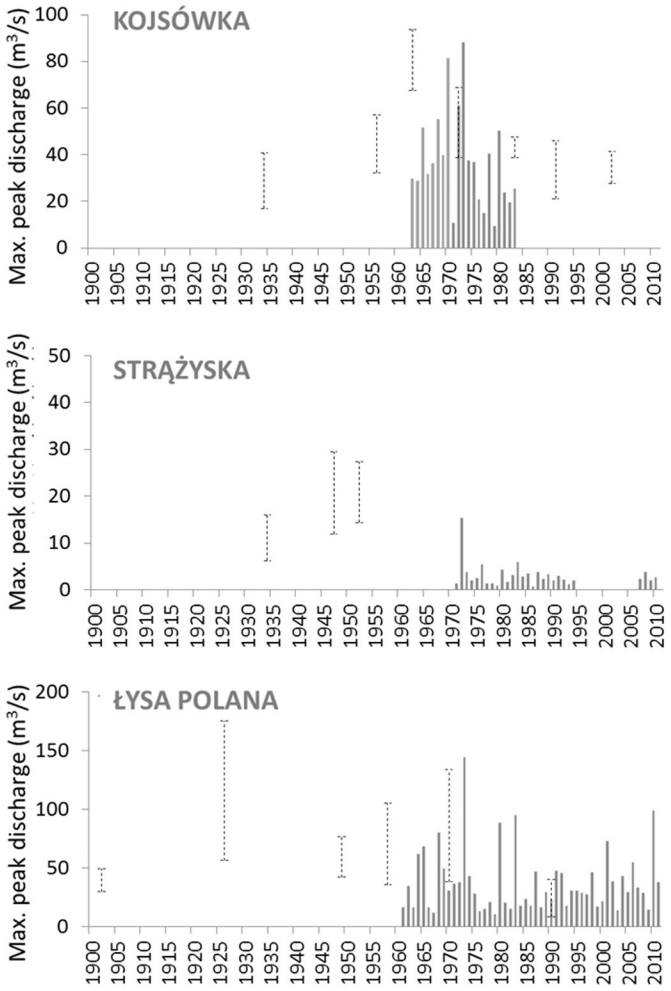

Fig. 6. Systematically recorded and reconstructed peak discharge series for each study site.

of the lack of continuous gauge records in the region. At the same time, we are confident that our approach based on geomorphology will limit the risk of large uncertainties in the peak discharge estimation resulting from incision–aggradation processes in the channel (e.g. Zawiejska and Wyżga, 2010; Wyżga et al., 2012), but clearly does not eliminate this problem fully. Several authors described the role of boulder transport (up to 0.2–0.6 m in 1973; Kaszowski and Kotarba, 1985) during historical events at the study sites, such that peak discharge reconstructions for events prior to the 1970s should be analysed and interpreted with caution.

The second source of uncertainty is related to the reliability of scar heights as PSI, especially in the case of old and partly hidden scars, which may lead to an over- and/or underestimation of maximum and mean scar heights. Gottesfeld and Gottesfeld (1990) reported that rubbing scars could form at positions located above the maximum flood stage as a consequence of deposits accumulating on tree stems. To resolve this problem, Ballesteros-Cánovas et al. (2011a) included a size-gradation classification of scars to correct this effect and to estimate peak discharge in ungauged mountain streams. In this study, we could not include a similar approach because of the limited number of tree samples available per event; consequently the peak discharge had to be estimated as an average of the estimates for all scarred trees. Moreover, it seems plausible that the mean height of scars might have been underestimated as wound closure rates are more important at the upper end of scars than in the lower parts (Schneuwly-Bollschweiler and Schneuwly, 2012). Finally, our results suggest that trees located in straight stream reaches or isolated trees growing on the internal side of channel bends at the bankfull level were the most suitable for discharge reconstructions (up to 20%). By contrast, trees standing in the central and external parts of the channel bends and trees growing in highly forested overbank locations were less useful for paleohydrological analyses.

5.2. Implication of the paleofloods in hazard assessment at Tatras

Historical archives describe the occurrence of intense floods triggered by summer precipitation events going back to the seventeenth century (Punzet and Czulak, 1988; Krzemień, 1991; Starkel, 1996; Kotarba, 2004). Flood risk, therefore, has been an important issue and known problem in the Tatra Mountains and their foreland for a long time; however, as a result of the highly fragmented and incomplete gauging network, interpretations have been rather difficult so far. The first gauging stations were installed in several streams and rivers in the Tatra Mountains foreland in the late nineteenth century. Theoretically, several important floods could have been recorded by the network, including the largest flood on record in 1934. However, the flood, as others in the twentieth century, not only completely destroyed several stations, but was also followed by the relocation of some crucial gauging stations such that comparison of events becomes difficult. In

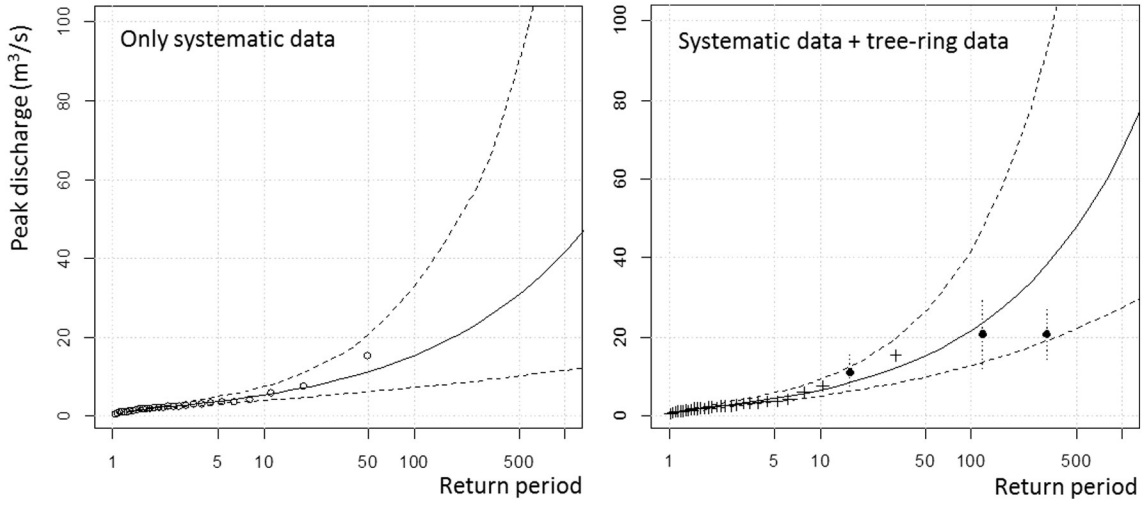

Fig. 7. Flood frequency distribution based on systematic flow-gauge series (1) and the series consisting of systematic flow data and the reconstructed paleodischarges (2).

Please cite this article as: Ballesteros-Cánovas, J.A., et al., Paleoflood discharge reconstruction in Tatra Mountain streams, Geomorphology (2015), http://dx.doi.org/10.1016/j.geomorph.2015.12.004

Table 4
Comparison of flood return period (T) estimates for Strążyska stream before and after including the reconstructed peak discharge. Presented values are obtained under the assumption of Xo = 20 m^3/s and h = 80 years, where "Xo" and "h" refers to the perception threshold (Xo) of a flood magnitude not exceeded during the period "h". Uncertainty is defined as the range of values between 95% and 5% CI. For more details, see Gáal et al. (2012).

Confidence interval (CI)	Estimated peak discharge (m^3/s)				Observed changes (%)			
	Systematic data		Systematic data and non-systematic data		In Q_{mean} (50%)		In uncertainties	
	T = 10 years	T = 100 years	T = 10 years	T = 100 years	T = 10 years	T = 100 years	T = 10 years	T = 100 years
95%	10.9	64.4	9.3	41.9				
Q_{mean} (50%)	6.0	17.2	6.6	21.6	10	25.5	−39.1	−47.3
5%	4.0	8.9	5.1	12.7				

addition, political instability of the region during the World Wars resulted in several changes of the gauging system and a partial loss of the documentation (Szczepański et al., 1996).

Our results also suggest that the reconstructed floods from the first half of the century were generally larger than those measured by the gauging stations during the second half of the twentieth century. This observation is in agreement with negative discharge trends in the foreland of the Tatra Mountains (Ruiz-Villanueva et al., 2014) probably reflecting the impact of intense forest recovery on runoff in the study region during the second half of the twentieth century (Wyżga et al., 2012). By contrast, the strong human impact from the eighteenth to the first half of the twentieth century resulted in increased soil erosion and surface runoff, thereby favouring the formation of braided channels. In addition, the reduction in sediment delivery was also favoured by the establishment of the national park and the related gradual cessation of pastoralism (i.e., 1955 in the case of RP and DR; 1970s in DCH; Grocholski, 2005).

This paper has demonstrated that the inclusion of nonsystematic paleohydrological data from tree-ring analysis can have an important impact on the results of flood frequency analysis. Our results highlight major changes in the Strążyska flow gauge (up to 25.5% for T = 100 years). These findings indicate that for this flow-gauge station, the flood hazard could be underestimated if systematic data is exclusively used to obtain flood frequency distribution. Therefore, the fact that our results are temporally contextualized in the last century and exclusively related with large events favours its use for the definition of future modelling scenarios and may limit drawbacks related with nonstationarity of flow behaviours on larger flow records or paleoflood reconstruction. However, the major finding here reported concerns the substantial reduction in the uncertainties in the estimation of a 100-year flood in all the flow gauge stations (see Table 4). This uncertainty should be stochastically included in future risk assessments in the area, as it has been done in other regions (Apel et al., 2004; McMillan and Brasington, 2008; Ballesteros-Cánovas et al., 2013). Finally, our peak discharge reconstruction could be used to deliver regional flood analysis given that the homogeneity test based on the Hosking and Wallis (2005) algorithm is satisfactory.

6. Conclusions

The magnitude of past flood events has been estimated for several Tatra Mountain streams using PSI in trees and the use of interactive two-dimensional hydraulic modelling, allowing us to extend the flow series until the early twentieth century. Most suitable trees for peak discharge reconstruction were located in straight stream reaches or isolated trees growing on the internal side of channel bends at the bankfull level. We have demonstrated that the inclusion of paleofloods from tree-ring reconstruction in the flow records resulted in an important change in the results of flood frequency analysis, in changes in the quantiles and a reduction of the related uncertainties. This change should be taken into account in future studies as epistemic uncertainty in infrastructure design and flood hazard delimitation.

Acknowledgements

This contribution has been realized in the framework of the FLORIST (Flood risk on the northern foothills of the Tatra Mountains) project, PSPB no. 153/2010, through a grant from Switzerland through the Swiss Contribution to the enlarged European Union. We appreciate the comments from anonymous reviewers and editors Bartlomiej Wyżga and Richard Marston, which have allowed improvement in the quality of this manuscript.

References

Apel, H., Thieken, A.H., Merz, B., Blöschl, G., 2004. Flood risk assessment and associated uncertainty. Nat. Hazards Earth Syst. 4 (2), 295–308.
Bac-Moszaszwili, M., Burchardt, J., Głazek, J., Iwanow, A., Jaroszewski, W., Kotański, Z., Lefeld, J., Mastella, L., Ozimkowski, W., Roniewicz, P., Skupiński, A., Westwalewicz-Mogilska, E., 1979. Mapa Geologiczna Tatr Polskich (Geological Map of the Polish Tatra), 1:30 000. Wydawnictwa Geologiczne, Warszawa, Poland.
Baker, V.R., 2008. Paleoflood hydrology: origin, progress, prospects. Geomorphology 101 (1), 1–13.
Ballesteros-Cánovas, J.A., Bodoque, J.M., Díez-Herrero, A., Sanchez-Silva, M., Stoffel, M., 2011b. Calibration of floodplain roughness and estimation of palaeoflood discharge based on tree-ring evidence and hydraulic modelling. J. Hydrol. 403, 103–115.
Ballesteros-Cánovas, J.A., Czajka, B., Janecka, K., Lempa, M., Kaczka, R.J., Stoffel, M., 2015b. Flash floods in the Tatra Mountain streams: frequency and triggers. Sci. Total Environ. 511, 639–648.
Ballesteros-Cánovas, J.A., Eguibar, M., Bodoque, J.M., Díez-Herrero, A., Stoffel, M., Gutiérrez-Pérez, I., 2011a. Estimating flash flood discharge in an ungauged mountain catchment with 2D hydraulic models and dendrogeomorphic paleostage indicators. Hydrol. Process. 25, 970–979.
Ballesteros-Cánovas, J.A., Rodriguez-Morata, C., Garófano-Gómez, V., Rubiales, J.M., Sánchez-Salguero, R., Stoffel, M., 2015c. Unravelling past flash flood activity in a forested mountain catchment of the Spanish Central System. J. Hydrol. 468-479.
Ballesteros-Cánovas, J.A., Sanchez-Silva, M., Bodoque, J.M., Díez-Herrero, A., 2013. An example of integrated approach to flood risk management: the case of Navaluenga (Central Spain). Water Resour. Manag. 27 (8), 3051–3069.
Ballesteros-Cánovas, J.A., Stoffel, M., Bodoque del Pozo, J.M., Bollschweiler, M., Hitz, O.M., Diez-Herrero, A., 2010. Changes in wood anatomy in tree rings of *Pinus pinaster* Ait. following wounding by flash floods. Tree-Ring Res. 66, 93–103.
Ballesteros-Cánovas, J.A., Stoffel, M., St. George, S., Hirschboeck, K., 2015a. A review of flood records from tree rings. Prog. Phys. Geogr. http://dx.doi.org/10.1177/0309133315608758.
Blöschl, G., Gaál, L., Hall, J., Kiss, A., Komma, J., Nester, T., et al., 2015. Increasing river floods: fiction or reality? Water Sci. Technol. 39 (9), 1–8.
Bodoque, J.M., Díez-Herrero, A., Eguibar, M.A., Benito, G., Ruiz-Villanueva, V., Ballesteros-Cánovas, J.A., 2015. Challenges in paleoflood hydrology applied to risk analysis in mountainous watersheds—a review. J. Hydrol. 529 (2), 449–467.
Borga, M., Anagnostou, E.N., Blöschl, G., Creutin, J.D., 2011. Flash flood forecasting, warning and risk management: the HYDRATE project. Environ. Sci. Pol. 14 (7), 834–844.
Borga, M., Stoffel, M., Marchi, L., Marra, F., Jakob, M., 2014. Hydrogeomorphic response to extreme rainfall in headwater systems: flash floods and debris flows. J. Hydrol. 518, 194–205.
Chow, V., 1959. Open-channel Hydraulics. McGraw-Hill, New York (680 pp.).
Corriell, F., 2002. Reconstruction of a Paleoflood Chronology for the Middlebury River Gorge Using Tree Scars as Flood Stage Indicators (PhD thesis) Middlebury College, USA.
Egginton, P.A., Day, T.J., 1977. Dendrochronologic investigation of high water events along Hodgson Creek, District of Mackenzie. Geol. Surv. Can. 77-1A, 381–384.
Enzel, Y., Ely, L.L., House, P.K., Baker, V.R., Webb, R.H., 1993. Paleoflood evidence for a natural upper bound to flood magnitudes in the Colorado River Basin. Water Resour. Res. 29 (7), 2287–2297.
Gaál, L., Szolgay, J., Kohnová, S., Hlavčová, K., Viglione, A., 2010. Inclusion of historical information in flood frequency analysis using a Bayesian MCMC technique: a case study for the power dam Orlík, Czech Republic. Contrib. Geophys. Geod. 40 (2), 121–147.

Gaume, E., Gaál, L., Viglione, A., Szolgay, J., Kohnová, S., Blöschl, G., 2010. Bayesian MCMC approach to regional flood frequency analyses involving extraordinary flood events at ungauged sites. J. Hydrol. 394 (1), 101–117.
Gottesfeld, A.S., 1996. British Columbia flood scars: maximum flood-stage indicator. Geomorphology 14, 319–325.
Gottesfeld, A.S., Gottesfeld, L.M.J., 1990. Floodplain dynamics of a wandering river, dendrochronology of the Morice River, British Columbia, Canada. Geomorphology 3, 159–179.
Grocholski, M., 2005. Pasterstwo w Tatrach (Pasture in Tatra Mountains). Tatry — Tatrzański Park Narodowy (Tatras — Tatra National Park) 4pp. 46–47 (in Polish).
Hosking, J.R.M., Wallis, J.R., 2005. Regional Frequency Analysis: An Approach Based on L-Moments. Cambridge University Press (224 pp.).
Jarrett, R.D., England, J.F., 2002. Reliability of paleostage indicators for paleoflood studies. In: House, P.K., Webb, R.H., Baker, V.R., Levish, D.R. (Eds.), Ancient Floods, Modern Hazards: Principles and Applications of Paleoflood HydrologyWater Science and Application vol. 5. American Geophysical Union, Washington, DC, pp. 91–109.
Kaszowski, L., Kotarba, A., 1985. Mapa współczesnych procesów morfogenetycznych [The map of recent morphogenetical precesses]. In: Trafas, K. (Ed.), Atlas Tatrzańskiego Parku Narodowego [Atlas of Tatra National Park]. Rada Tatrzanskiego Parku Narodowego, Zakopane-Kraków (in Polish).
Knighton, D., 2014. Fluvial forms and processes: a new perspective. Routledge, New York (384 pp.).
Kotarba, A., 2004. Zdarzenia geomorfologiczne w Tatrach Wysokich podczas małej epoki lodowej (Geomorphic events in the High Tatra Mountains during the Little Ice Age). In: Kotarba, A. (Ed.), Rola małej epoki lodowej w przekształcaniu środowiska przyrodniczego Tatr. (Effect of the Little Ice Age on Transformation of Natural Environment of the Tatra Mountains). IGiPZ PAN, Kraków, pp. 9–55 (in Polish, with English summary).
Krzemień, K., 1991. Dynamika wysokogórskiego systemu fluwialnego na przykładzie Tatr Zachodnich (Dynamics of the high-mountain fluvial system with the Western Tatra Mts. as example). Rozprawy Habilitacyjne 215. Uniwersytet Jagielloński, Kraków, pp. 1–160 (in Polish, with English summary).
Kundzewicz, Z.W., Hirabayashi, Y., Kanae, S., 2010. River floods in the changing climate—observations and projections. Water Resour. Manag. 24 (11), 2633–2646.
Kundzewicz, Z., Stoffel, M., Kaczka, R., Wyżga, B., Niedźwiedź, T., Pińskwar, I., Ruiz-Villanueva, V., Łupikasza, E., Czajka, B., Ballesteros-Cánovas, J., Małarzewski, Ł., Choryński, A., Janecka, A., Mikuś, P., 2014. Floods at the northern foothills of the Tatra Mountains—a Polish–Swiss research project. Acta Geophys. 62 (3), 620–641.
Lang, M., Ouarda, T.B.M.J., Bobée, B., 1999. Towards operational guidelines for over-threshold modeling. J. Hydrol. 225 (3), 103–117.
Marchi, L., Borga, M., Preciso, E., Gaume, E., 2010. Characterisation of selected extreme flash floods in Europe and implications for flood risk management. J. Hydrol. 394 (1), 118–133.
McCord, V.A., 1996. Fluvial process dendrogeomorphology: reconstruction of flood events from the southwestern United States using flood-scarred trees. In: Dean, J.S. (Ed.), Tree-ring, Environ. Humanity: Radiocarbon, pp. 689–699.
McMillan, H.K., Brasington, J., 2008. End-to-end flood risk assessment: a coupled model cascade with uncertainty estimation. Water Resour. Res. 44 (3). http://dx.doi.org/10.1029/2007WR005995.
Merz, B., Aerts, J., Arnbjerg-Nielsen, K., Baldi, M., Becker, A., et al., 2014. Floods and climate: emerging perspectives for flood risk assessment and management. Nat. Hazards Earth Syst. 14 (7), 1921–1942.
Niedzwiedz, T., 1992. Climate of the Tatra Mountains. Mt. Res. Dev. 12 (2), 131–146.
Niedźwiedź, T., Łupikasza, E., Pińskwar, I., Kundzewicz, Z.W., Stoffel, M., Małarzewski, Ł., 2015. Variability of high rainfalls and related synoptic situations causing heavy floods at the northern foothills of the Tatra Mountains. Theor. Appl. Climatol. 119 (1–2), 273–284.
O'Connell, D.R.H., 2005. Nonparametric Bayesian flood frequency estimation. J. Hydrol. 313, 79–96.
O'Connor, J.E., Ely, L.L., Wohl, E.E., Stevens, L.E., Melis, T.S., Kale, V.S., Baker, V.R., 1994. A 4500-year record of large floods on the Colorado River in the Grand Canyon, Arizona. J. Geol. 102, 1–9.
Punzet, J., Czulak, J., 1988. Bilanse odplywu wielkich wezbran górnej Wisly w XX wieku. Wiad. IMGW 11 (3–4), 3–16.
Ruiz-Villanueva, V., Díez-Herrero, A., Bodoque, J.M., Ballesteros-Cánovas, J.A., Stoffel, M., 2013. Characterisation of flash floods in small ungauged mountain basins of Central Spain using an integrated approach. Catena 110, 32–43.
Ruiz-Villanueva, V., Stoffel, M., Wyżga, B., Kundzewicz, Z.W., Czajka, B., Niedźwiedź, T., 2014. Decadal variability of floods in the northern foreland of the Tatra Mountains. Reg. Environ. Chang. http://dx.doi.org/10.1007/s10113-014-0694-9.
Schneuwly-Bollschweiler, M., Schneuwly, D.M., 2012. How fast do European conifers overgrow wounds inflicted by rockfall? Tree Physiol. 32, 968–975.
Sigafoos, R.S., 1964. Botanical evidence of floods and flood-plain deposition. US Geol. Surv. Prof. Pap. 485A (35 pp.).
Smith, D.G., Reynolds, D.M., 1983. Trees scars to determine the frequency and stage of high magnitude river ice drives and jams, Red Deer, Alberta. Can. Water Resour. J. 8 (3), 77–94.
Starkel, L., 1996. Geomorphic role of extreme rainfalls in the Polish Carpathians. Stud. Geomorphol. Carpatho Balc. 30, 21–39.
Stoffel, M., Corona, C., 2014. Dendroecological dating of geomorphic disturbance in trees. Tree-Ring Res. 70, 3–20.
Stoffel, M., Wilford, D.J., 2012. Hydrogeomorphic processes and vegetation: disturbance, process histories, dependencies and interactions. Earth Surf. Process. Landf. 37 (1), 9–22.
Szczepański, W., Czarnecka, H., Mierzwiński, A., 1996. Atlas posterunków wodowskazowych dla potrzeb państwowego monitoringu środowiska: posterunki wodowskazowe IMGW. PIOŚ.
Trappmann, D., Stoffel, M., 2015. Visual dating of rockfall scars in *Larix decidua* trees. Geomorphology 245, 62–72.
Viglione, A., Hosking, J.R., Laio, F., Miller, A., et al., 2013. Package 'nsRFA'. Non-supervised Regional Frequency Analysis. CRAN Repository (http://r.adu.org.za/web/packages/nsRFA/nsRFA.pdf).
Webb, R.H., Jarrett, R.D., 2002. One-dimensional estimation techniques for discharges of paleofloods and historical floods. In: House, P.K., Webb, R.H., Baker, V.R., Levish, D.R. (Eds.), Ancient Floods, Modern Hazards: Principles and Applications of Paleoflood HydrologyWater Science and Application vol. 5. American Geophysical Union, Washington, DC, pp. 111–125.
Williams, G.P., 1978. Bankfull discharge of rivers. Water Resour. Res. 14 (6), 1141–1154.
Wohl, E., 2000. Mountain rivers. No. 14. Amer. Geophysical Union, Washington, D. C. (320 pp.).
Wohl, E., 2006. Human impacts to mountain streams. Geomorphology 79 (3), 217–248.
Wyżga, B., 1997. Methods for studying the response of flood flows to channel change. J. Hydrol. 198, 271–288.
Wyżga, B., Zawiejska, J., Radecki-Pawlik, A., Hajdukiewicz, H., 2012. Environmental change, hydromorphological reference conditions and the restoration of Polish Carpathian rivers. Earth Surf. Process. Landf. 37 (11), 1213–1226.
Yanosky, T.M., Jarrett, R.D., 2002. Dendrochronologic evidence for the frequency and magnitude of paleofloods. In: House, P.K., Webb, R.H., Baker, V.R., Levish, D.R. (Eds.), Ancient Floods, Modern Hazards: Principles and Applications of Paleoflood HydrologyWater Sci. Appl. vol. 5. Amer. Geophysical Union, Washington, DC, pp. 77–89.
Zawiejska, J., Wyżga, B., 2010. Twentieth-century channel change on the Dunajec River, southern Poland: patterns, causes and controls. Geomorphology 117 (3), 234–246.

Please cite this article as: Ballesteros-Cánovas, J.A., et al., Paleoflood discharge reconstruction in Tatra Mountain streams, Geomorphology (2015), http://dx.doi.org/10.1016/j.geomorph.2015.12.004